*Int. J. Electrochem. Sci.*, 17 **(2022)** Article Number: 220951, doi: 10.20964/2022.09.65

International Journal of
ELECTROCHEMICAL
SCIENCE
www.electrochemsci.org

# Effect of Thermal Parameters on Behaviour of A Lithium-Ion Battery: Simulation Study

*Jackleen S. Same, A. El-Tayeb*[*]*, Ibrahim Moukhtar, Esam H. Abdelhameed, Adel Z. El-Dein*

Electric Engineering Department, Faculty of Energy Engineering, Aswan University, Aswan, Egypt.
[*]E-mail: Ahmed_al_tayeb@aswu.edu.eg

*Received:* 20 January 2022 / *Accepted:* 21 June 2022 / *Published:* 7 August 2022

Lithium-Ion battery temperature should maintain within a specific range during charging and discharging processes to ensure the higher performance of the battery, longer life of the battery, and safety of use. Accordingly, a battery cooling system is required. In general, generated heat through chemical reactions within the battery is the main source of battery temperature increment. The generated heat which spreads throughout the battery components and surface is affected by many factors such as the ambient temperature, the type of materials used, and the design dimensions. Hence, there is more than one methodology to control the temperature of the battery. These methods include the use of cooling systems, controlling the design dimensions, and using various types of materials for battery components. The main core of this article is to establish a simulation program implemented by Finite Element Method (FEM) to examine the impact of variation of some operating and thermal factors on the battery thermal operation. These parameters are ambient temperature (255.4, 277.6, 299.9, 322.1, 344.3 K), discharge/charge rates (0.5C, 1C, 1.5C, 2C). Heat transfer coefficient, thermal conductivity, density, and heat capacity are some of the thermal attributes of the employed material.

**Keywords**: Battery Thermal Management Systems, Thermal Parameters, Cooling, Batteries, Simulation of Lithium-Ion Batteries,

## 1. INTRODUCTION

In the last years, lithium-ion (Li-ion) batteries have attracted attention as a common power source in electric vehicles and portable electronic devices due to their many advantages. In lithium-ion batteries (LIBs), the thermal conductivities of separators, electrolytes, cathodes, and anodes are critical in determining thermal energy transfer. Although LIBs offer several benefits, including enhanced safety performance, high energy density, and long service life, there are growing concerns regarding their safety [**1**–**5**]. On the other hand, the heat produced inside the battery rises fast as the energy density rises and the volume shrinks. The Joule heat and the exothermic electrochemical reaction produced by the current during charging and discharging are the major sources of heat. If the battery's internal heat transfer

performance is poor, the efficiency of heat dissipation is inadequate, which might result in thermal stress and regional heating. This will have a major influence on the battery's performance and may even result in thermal runaway [**6-7**]. Weak lithium transfer kinetics and small electrolyte conductivity of the battery cause capacity loss at low temperatures. The high operating temperature may result in a loss of battery energy as well as safety concerns. The battery capacity declines over cycles as the operating temperature rises due to the loss of active material [**8-9**]. The overheating that occurs in a battery during the run-off period is split into double components: revisable heat and irreversible heat. This total heat is the main reason for the high temperature. There are many risks due to the high temperature of the battery, which gets damaged and may lead to an explosion, which brings many risks to human life and the environment. Therefore, there is much research on how to improve the efficiency of the battery by external or internal cooling [**10-12**]. In this paper, the LIBs are considered, which have been widely used, especially recently, as the main storage device in many vital applications because of their great energy storage capacity, economic competence, low self-discharge, and small size compared to other battery types. Cylindrical cells, such as the 18650s, are commonly used in home electrical devices, power tools, and electric cars [**13**]. Hence, in this study, the investigation of how to reduce the battery temperature by changing some thermal parameters during the charging and discharging process at different ambient temperatures is presented and discussed. The cylindrical battery cell:18650s is simulated in this study as a standard model to research the thermal performance of LIBs. Simulation model created by FEM in Two Dimensions 2D to examine the thermal behavior of LIBs in various air-cooling conditions and contains a lumped battery model to simulate the chemistry of battery cells. Using the multiphase coupling node Electrochemical Heating, the two models are linked by the produced heat source and average temperature. The effects of discharge rate and thermal parameters are studied individually to see how the change of each parameter affects the improvement of battery efficiency, especially the reduction of temperature.

## 2. SIMULATION METHODS

Numerical simulations are progressively have been utilized in numerous battery design evaluations as computer science advances. Numerical simulation confirms experiment results using fewer physical resources than normal experiments and also shows in-depth essential performance characteristics such as temperature, pressure, and electrochemical properties. Furthermore, the internal battery system can be viewed to properly detect issues that might be resulting in battery component failure. The creation of numerical battery models has benefited in a better understanding of the underlying principles of the battery circuit and their influence on the environment [**14**]. In the study of battery properties and the operation of batteries, mathematical models have been frequently employed. To build and optimize the batteries, a precise mathematical model must be developed. The simulation results give comprehensible data about the battery's functioning. An appropriate mathematical model can define and govern parameter modification for a few parameters that are unknown empirically. For tortuosity or liquid-phase transport resistance, direct experimental data is required, for example, is absent; nevertheless, mathematical models may be used to mimic these properties [**15**]. The effect of temperature and heat dispersion on battery packs has been studied by several researchers [**16**]. To

determine heat production, Sherfey et al [**18**], Gross et al [**19**], Dibrov et al [**20**], and Chen et al [**21**] employed experimental methods using calorimeters. In addition, Li [**22**] created 2D Computational Fluid Dynamics (CFD) models to undertake comprehensive simulations of thermal management difficulties inside an air-cooled battery pack. The previous study focused on the industrial battery modules analysis and aided in the thermal control of Li-ion batteries. However, it has been shown that fewer studies have been undertaken in terms of distinct cell layouts and inter-cell distance factors [**16**]. The requirement to tackle complicated structural and elasticity analysis issues in engineering led to the development of FEM methodologies and theories [**23**]. Many FEM software, including RADIOSS, ABAQUS, and LS-DYNA, where RADIOSS is a versatile finite element solver by Altair Engineering. It can solve both linear and non-linear problems. It is a finite element solver that handles engineering problems ranging from linear statics and linear dynamics to nonlinear transient dynamics and mechanical systems using implicit and explicit integration methodologies. ABAQUS; ABAQUS is a finite element analysis and computer-aided engineering software package that was first launched in 1978. The abacus calculation instrument inspired the name and logo of this program, and LS-DYNA; LS-DYNA is a multi-purpose finite element program capable of simulating complex real-world problems. The automobile, aerospace, construction, military, manufacturing, and bioengineering industries also employ it. All these programs were utilized to simulate the material composition, and this approach was developed and employed in analyzing mechanical characteristics. CFD is a useful tool for studying various thermal fluid energetic factors and simulating various physics fields [**23–25**]. CFD allows the user to utilize the equations that govern fluid flow for a wide variety of complicated conditions, offering equally quantitative and insight predictions. CFD modeling may offer extensive information on the thermal and electrical fields in the battery that is challenging to examine using experimental methods [**14**]. The results of a cylindrical lithium-ion battery's FEA are provided [**24**]. The model was simplified by using cylindrical coordinates and lumped modeling theories. The Li-ion One Dimension (1D) model was also utilized to establish the precise quantity of heat produced by a battery cell [**25**]. For the cell temperature distribution, the 1D model is combined with a three Dimension (3D) model. The energy conservation rule is used to generate the energy equilibrium Equation (1) for cylindrical LIBs, which may be represented as follows [**16**]:

$$\rho C_p \frac{\partial T}{\partial t} = \frac{1}{r}\frac{\partial}{\partial r}\left(K_r r \frac{\partial T}{\partial r}\right) + \frac{1}{r^2}\frac{\partial}{\partial \varphi}\left(K_a \frac{\partial T}{\partial r}\right) + \frac{\partial}{\partial z}\left(K_z \frac{\partial T}{\partial z}\right) + \dot{Q} \quad (1)$$

Where $\rho$ is the density of active battery material ($kg/m^3$) and $C_p$ stands for specific heat capacity ($J/kg\ K$). The absolute temperature is denoted by $T$ ($K$), while the radius of the battery cell is denoted by $r$ (m). The $z$ directions ($W/mK$) are denoted as $k_r$, $k_a$, and $k_z$, and the thermal conductivity in the radial, axial. Furthermore, $\dot{Q}$ signifies the battery cell's volumetric heat production rate ($W$). The phrase on the left indicates the stored energy in the cell, while the phrases on the right show the volumetric heat production ratio expressions and 3D heat conduction, in that order. The article's structure is as follows: first, the simulation program based on the FEM technique and a lumped model of one battery is employed, in section 2. Section 3 discusses the influence of temperature on a single cell of LIBs. Section 4 discusses the influence of the heat transport and thermal parameters of a Li-ion cell module. The description of the thermal model is demonstrated in section 5. In section 6, the simulation results were discussed. Finally, the conclusion was presented.

## 3. EFFECT OF TEMPERATURE

Heat production, and hence thermal transfer, is vital in assuring LIBs safety, performance, and longevity. The most major aging accelerator is a rise in battery temperature [**26**]. The cathode, anode, separator, electrolyte, and collector are the key elements of LIBs. The risk of thermal runaway increases due to any problem within any element of the battery components, like poor bonding strength which permits the electrolyte to wear away the electrode or melting separator consequently producing short-circuit inside the battery. High temperature promotes the increase of the interface layer of the solid electrolyte and raises internal resistance that minimizes energy delivery [**27-29**]. The three types of causes of thermal runaway are electrical abuse, thermal abuse, and mechanical abuse. The first one is that LIBs are susceptible to overcharging and short-circuiting, which can result in electrical abuse. In the second, exterior heat causes, or inside electrochemical side reactions can cause thermal runaway in LIBs, resulting in thermal runaway. Finally, LIBs are stressed externally, their shell deforms or even penetrates, resulting in mechanical damage as shown in Figure (1).

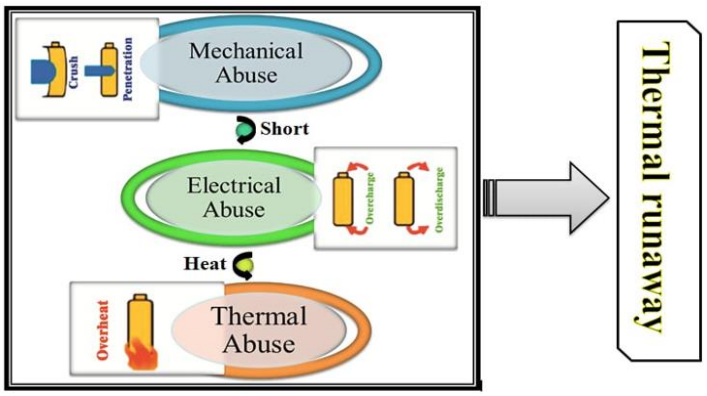


**Figure 1.** Li-ion battery thermal runaway sources

All mentioned abuses will produce a sequence reaction in the lithium-ion cell in a short time period, causing the internal battery temperature to quickly increase. Consequently, this leads to thermal runaway and generally results in smoke, fire, and even explosion. As a result, it is critical to keep an eye on lithium-ion batteries' thermal runaway [**30-3**2]. The major duties of Battery Thermal Management Systems (BTMS) might include maintaining a certain temperature range and a consistent temperature differential. So, the main factor directly influencing the efficiency and lifetime of the cell is the battery temperature as well as the normal temperature that batteries run between 25˚C and 40˚C for the most effective behavior. Less or more than the allowed range of the temperature may affect the efficiency and battery life; therefore, the temperature must be maintained at the safe limits [**33-34**]. It's important to standardize battery temperature because it has a powerful effect on the accessibility of discharge and energy charging, battery stabilizing, and charging admission through regenerative braking. A significant difference in the battery pack temperature be able to various cells charging and unloading at different rates and leads to electrically unstable cells and reduce battery pack behavior. Self-discharge also has a long-term effect, and it leads to a reduction in the state of effective operation, and thermal aging and cyclic determines battery life.

## 4. HEAT TRANSFER AND THERMAL PROPERTIES

The term "heat transfer" refers to the transmission of thermal energy, which is the temperature difference between two points in space. There are three different modes for the transfer of heat, namely: conduction, convection, and radiation, as shown in Figure (2). To begin, conduction refers to the transport of heat via a solid medium (solid) or a fluid when the medium has a temperature differential. Second, convection refers to the transfer of heat from a flowing fluid to a solid. Lastly, when a material is surrounded by differing temperatures, the transport of heat by electromagnetic waves is known as radiation [**35**].

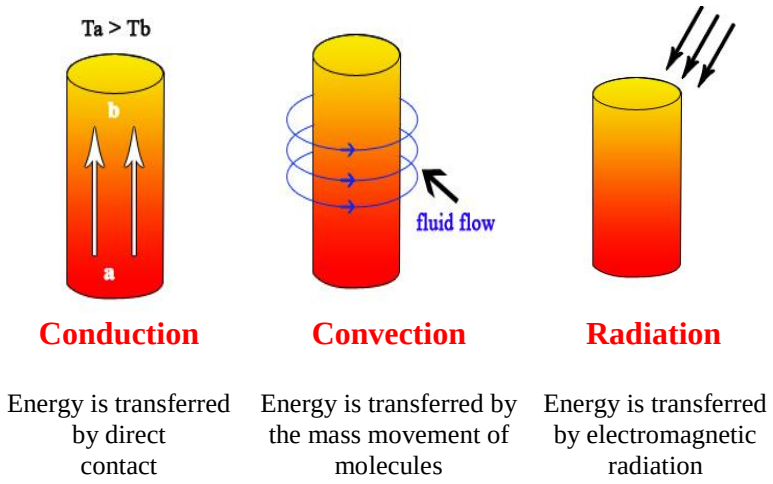


**Figure 2.** Different heat transfer mechanisms in Li-ion batteries

The heat of reaction, ohmic heat, reverse and external heat contact resistance temperature are sources of heat in a battery that occur from a chemical reaction that leads to heat creation by the transport of electrons or from the electrode during charging and discharging. The heat of the reaction is divided into reversible and irreversible heat, the total resistive heat production is caused by the electrolyte and ohmic resistance in the solid active materials, as shown in Figure (3). The entropy changes of the cathode and anode are responsible for the total reversible heat generation, while the contact resistance between the cell terminals and the external connection is responsible for the final heat component [**36**]. Equation (2) refers to the total heat produced from the battery, which is divided into two parts. The first segment is mostly caused by joule heating resistance, whereas the second is caused by entropy change during charge or discharge.

$$Q = Q_{irr} + Q_{rev} = I.(V - U_{ouc}) + I.T.\frac{\partial U_{ouc}}{\partial T} \quad (2)$$

where $\boldsymbol{Q}$ is heat of the reaction, $\boldsymbol{Q_{rev}}$ is reversible heat and $\boldsymbol{Q_{irr}}$ is irreversible heat. The discharge current is $\boldsymbol{I}$, the cell potential is $\boldsymbol{V}$, the battery temperature is $\boldsymbol{T}$, the open circuit potential is $\boldsymbol{U_{ouc}}$, and the Entropic Heat Coefficient (EHC) is $\boldsymbol{\partial U_{ouc}/\partial T}$ .This section of Equation (3) is dependent on the cell overpotential, $\boldsymbol{U_{ouc}}$, and the difference between $\boldsymbol{V}$ and $\boldsymbol{I}$, such as joule heating within the battery, and it refers to the irreversible heat owing to internal resistance and the energy expended in electrode

overpotentials and means irreversible process. The value of this part of the equation is always considered to be positive.

$$E_d = Q.\Delta t \tag{3}$$

Where $\boldsymbol{E_d}$ is the expended energy in electrode overpotentials, $\boldsymbol{Q}$ is heat of the reaction, and $\boldsymbol{\Delta t}$ is the time interval.

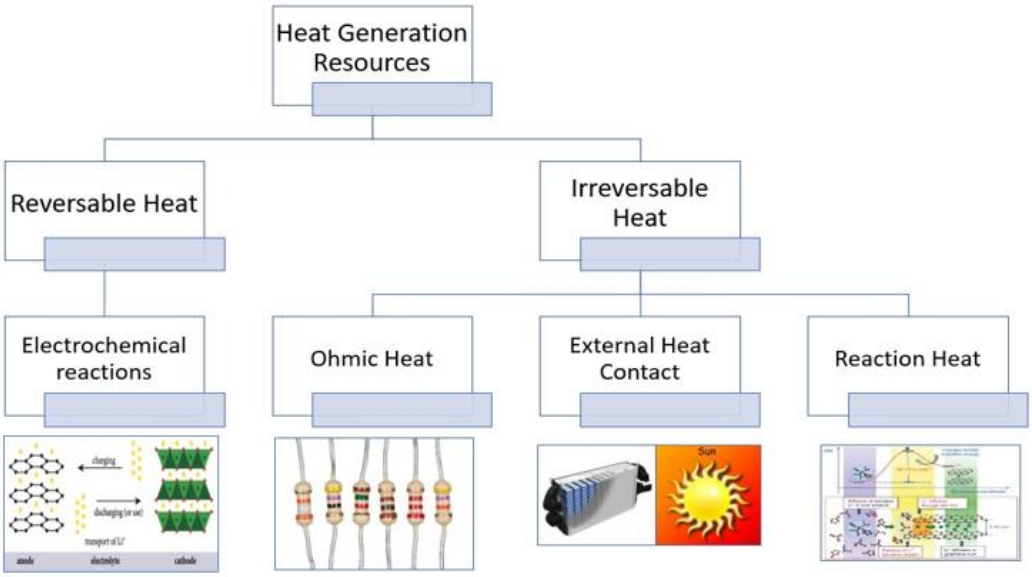


**Figure 3.** Heat generation resources

## 5. THERMAL MODEL DESCRIPTION

The parameters of the battery are very important for defining the battery explicitly in terms of the dimensions, size, and shape of the battery as well as the heat transfer coefficient and many others as shown in the following paragraphs. All the fixed and variable parameters of the battery to make it easier for the program used to complete the simulation to read them and to make it clear to everyone who reads that research. The electrochemical roles of the electrodes reverse between anode and cathode, depending on the direction of current flow through the cell. The details of geometry and properties of battery or parameters used in this study are given in Table.1. This research studies the effect of changing some parameters on the thermal behavior of the battery and creating an advanced model through which the battery efficiency can be updated, and that is what we hope to reach in the upcoming studies. Hence, in this study, the investigation of how to reduce the battery temperature by changing some thermal parameters during the charging and discharging process at different ambient temperatures is presented and discussed. The cylindrical battery cell: 18650s is simulated in this study as a standard model to research the thermal performance of LIBs. Simulation model created by FEM in 2D to examine the thermal behavior of LIBs in various air-cooling conditions and contains a lumped battery model to simulate the chemistry of battery cells. Using the multiphase coupling node Electrochemical Heating, the two models are linked by the produced heat source and average temperature.

**Table 1.** Parameters of 18560 cylindrical li-ion battery

| Parameter Description | Value | |
|---|---|---|
| Thickness of battery canister, $d_{can}$ | 0.25 | mm |
| Battery radius, $r_B$ | 9 | mm |
| Battery height, $h_B$ | 65 | mm |
| Mandrel radius, $r_m$ | 2 | mm |
| Length of negative electrode, $l_{nE}$ | 55 | μm |
| Length of separator, $l_s$ | 30 | μm |
| Length of positive electrode, $l_{pE}$ | 55 | μm |
| Negative current collector thickness, $l_{nCC}$ | 7 | um |
| Positive current collector thickness, $l_{pCC}$ | 10 | um |
| Positive electrode thermal conductivity, $k_{T\_p}$ | 1.58 | W/(m·K) |
| Negative electrode thermal conductivity, $k_{T\_n}$ | 1.04 | W/(m·K) |
| Positive current collector thermal conductivity, $k_{T\_pCC}$ | 170 | W/(m·K) |
| Negative current collector thermal conductivity, $k_{T\_nCC}$ | 398 | W/(m·K) |
| Separator thermal conductivity, $k_{T\_s}$ | 0.344 | W/(m·K) |
| Positive electrode density, $r_{ho\_p}$ | 2328.5 | kg/m$^3$ |
| Negative electrode density, $r_{ho\_n}$ | 1347.33 | kg/m$^3$ |
| Positive current collector density, $r_{ho\_pCC}$ | 2770 | kg/ m$^3$ |
| Negative current collector density, $r_{ho\_nCC}$ | 8933 | kg/ m$^3$ |
| Separator density, $r_{ho\_s}$ | 1008.98 | kg/ m$^3$ |
| Positive electrode heat capacity, $C_{pp}$ | 1269.21 | J/(kg·K) |
| Negative electrode heat capacity, $C_{pn}$ | 1437.4 | J/(kg·K) |
| Positive current collector heat capacity, $C_{ppCC}$ | 875 | J/(kg·K) |
| Negative current collector heat capacity, $C_{pnCC}$ | 385 | J/(kg·K) |
| Separator heat capacity, $C_{ps}$ | 1978.16 | J/(kg·K) |
| Cycle time, $t_c$ | 600 | s |
| Inlet temperature, $T_{in}$ | 298.15 | K |
| Cell capacity, $Q_B$ | 1.258 | A·h |
| Ohmic overpotential at 1C, $\zeta_{1C}$ | 4.5 | mV |
| Dimensionless charge exchange current, $J_0$ | 0.85 | |
| Diffusion time constant, $\tau$ | 1000 | s |
| Initial state-of-charge, $SOC_i$ | 0.2 | |
| Applied current, $I_{\text{app}}$ | 2.5 | A |
| the rate of discharge/charge, $C_r$ | 1 | |
| Time of discharge, $t_{\text{d}}$ | 3600/$C_r$ | s |
| Cell thickness, $l_B$ | Given by Eq. (4) | |
| Battery thermal conductivity, angular, $k_{T\_Ba}$ | Given by Eq. (5) | |
| Battery thermal conductivity, radial, $k_{T\_Br}$ | Given by Eq. (6) | |
| Battery density, $r_{ho\_B}$ | Given by Eq. (7) | |
| Battery heat capacity, $C_{pB}$ | Given by Eq. (8) | |
| Initial temperature, $T_i$ | 25 $C$ | |

$$l_B = l_n + l_{nCC} + l_s + l_p + l_{pCC} \tag{4}$$

$$k_{T\_Ba} = (k_{T\_p} \cdot l_p + k_{T\_n} \cdot l_n + k_{T\_pCC} \cdot l_{pCC} + k_{T\_nCC} \cdot l_{nCC} + k_{T\_s} \cdot l_s)/l_B \tag{5}$$

$$k_{T\_Br} = l_B / \left( \frac{l_p}{k_{T\_p}} + \frac{l_n}{k_{T\_n}} + \frac{l_{pCC}}{k_{T\_pCC}} + \frac{l_{nCC}}{k_{T\_nCC}} + \frac{l_s}{k_{T\_s}} \right) \quad (6)$$

$$r_{ho\_B} = (r_{ho\_p} \cdot l_p + r_{ho\_n} \cdot l_n + r_{ho\_pCC} \cdot l_{pCC} + r_{ho\_nCC} \cdot l_{nCC} + r_{ho\_s} \cdot l_s)/l_B \quad (7)$$

$$C_{pB} = (C_{pp} \cdot l_p + C_{pn} \cdot l_n + C_{ppCC} \cdot l_{pCC} + C_{pnCC} \cdot l_{nCC} + C_{ps} \cdot l_s)/l_B \quad (8)$$

The effects of discharge rate and thermal parameters are studied individually to see how the change of each parameter affects the improvement of battery efficiency, especially the reduction of temperature. Simulation of 18560 LIB's are made by changing some of the thermal parameters or thermal properties of the used material such as: Heat Transfer Coefficient $h$ $[W.m^2.k]$, Thermal Conductivity $k$ $(W.m^{-1}.k^{-1})$, Density $D$ [kg/m$^3$], and Heat Capacity $C_p$ (J/Kg). Studying the LIB's performance in the different cases which change the thermal parameters together to achieve the best case in improving the thermal behavior in battery, the thermal properties set the following data (charging & discharging battery $C_r$ (2.5C), heat capacity of battery $C_{pB}$ (3560 J/Kg), resistivity of battery $r_{ho\_B}$ (1114.6), thermal conductivity of separator $k_{T\_s}$ $(W.m^{-1}.k^{-1})$).

## 6. SIMULATION RESULTS AND DISCUSSION

In this paper, a simulation program based on FEM was used to create the battery model in 2D with axial symmetry. The LIBs consist of three parts as follows: the first is the anode, which is the negative conductor and made from carbon $LiC_6$ that corresponds to a peak capacity of 372 mAh/g. The second is the cathode, which is the positive electrode and is typically a metallic oxide $LiCoO_2$ and $LiMn_2O_4$. The third is the lithium salt electrolyte in an organic solvent ($LiPF_6$) [**37-41**]. Furthermore, the model comprises three domains: (1) active battery material domain; (2) mandrel; (3) cylindrical battery connector. Set an alternating charge/discharge current of one cycle with a duration of 600 s and a relaxation phase of 3600 s using the square wave function at a temperature of 298.15 K, the heat transfer coefficient is $h$ = 20 W/(m$^2$.K), as illustrated in Figure (4-a). The impacts of varied discharge–charge ratios on temperature are compared in this section. The appropriate conclusions may be drawn from the battery's partial charge and discharge simulation, this is more in keeping with the real-world situation, when the battery is not fully charged and drained while in use. Cell State of Charge SOC change with time was presented in Figure (4-b). The average and maximum temperature rises of the cell are presented based on the simulated data. As shown in Figure (5), the illustration of the highest, average, and minimum temperatures of the cell throughout the simulation indicates that the difference among the three readings is less than 0.75 K. As demonstrated in figures, the greatest temperature is found in the effective cell material in the center of the cell at 3600 s. In this article, the influence of the different parameters in the LIBs thermal performance is investigated separately and integrated to enhance the thermal properties of the cell.

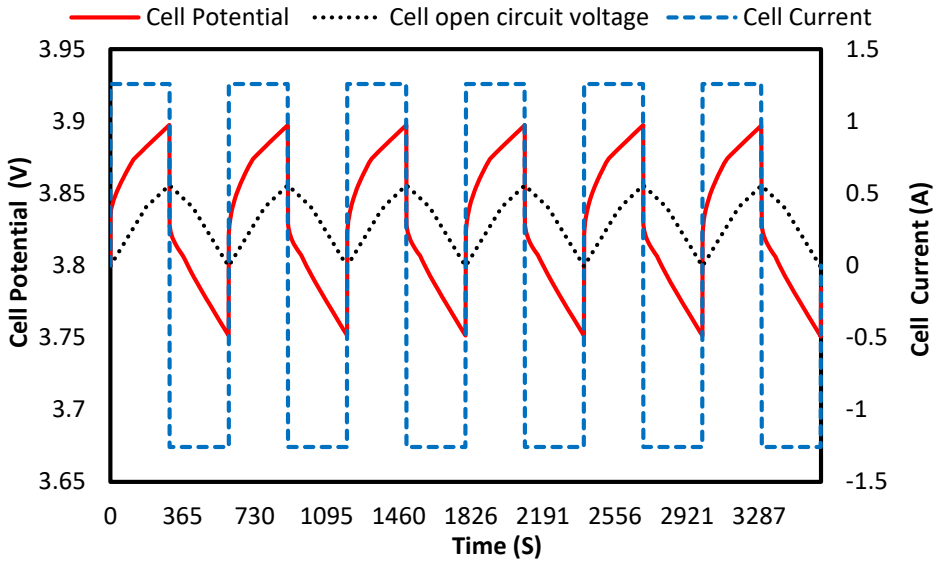


(a) Potential, open circuit voltage and current of the battery with time.

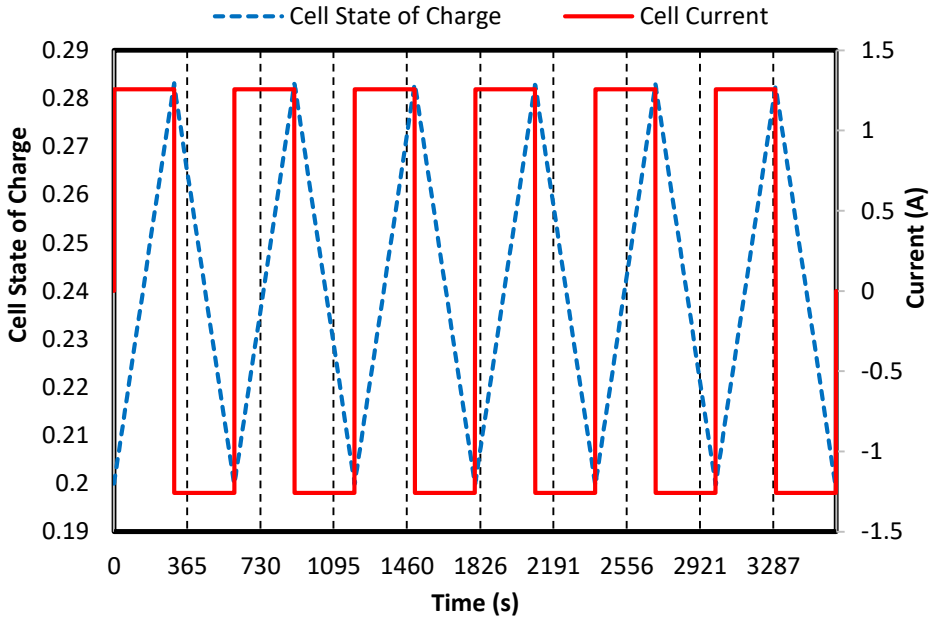


(a) Cell State of Charge SOC and current of the battery with time.

**Figure 4.** Battery performance with relaxation time 3600 s using the square wave function.

The parameters under study include the constant current discharge, state of charge, heat transfer coefficient, thermal conductivity, heat capacity, density. Different values of these parameters are investigated to find out which parameters have an effective effect for improving the thermal properties of the battery or what kind of noticeable change is at this point. The flow temperature varies between 298 and 314 K. The maximum temperature is given at the mandrel and active battery material. The cell's outside boundary has the lowest temperature since it is in contact with the wind, as indicated by the shaded plot for the temperature in Figure (6). In the following lines, the simulation results for different parameters that influence the thermal performance of lithium-ion cells such as constant current discharge, thermal conductivity, state of charge, heat transfer coefficient, heat capacity, and density are presented.

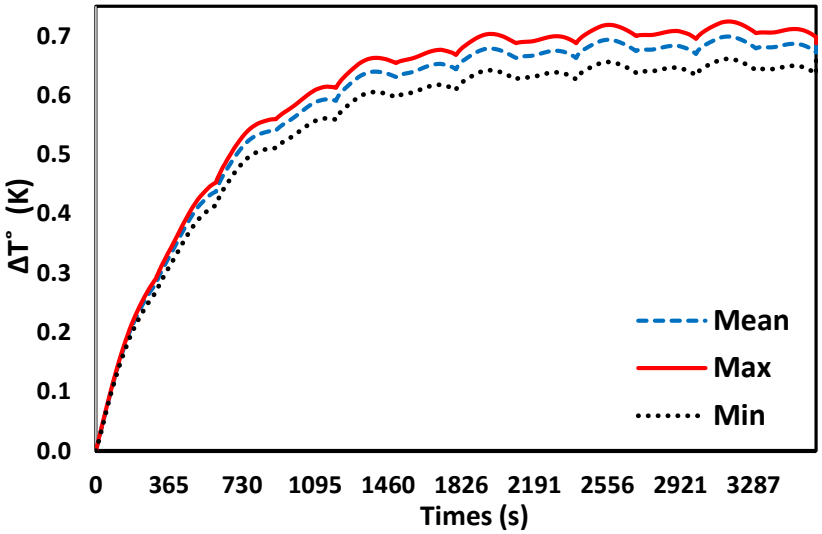


**Figure 5.** Mean, maximum, and minimum temperatures

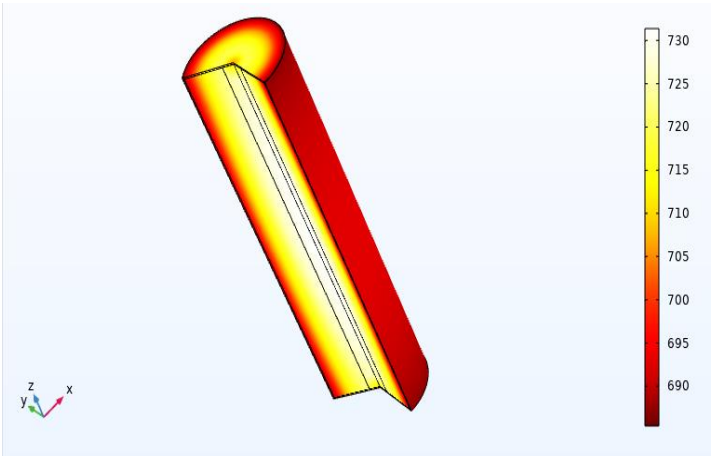


(a) Temperature distribution (Surface) at $C_r = 0.5$, $t = 0$ , $SOC_i = 1$, and $I_{\text{app}} = 1.25$

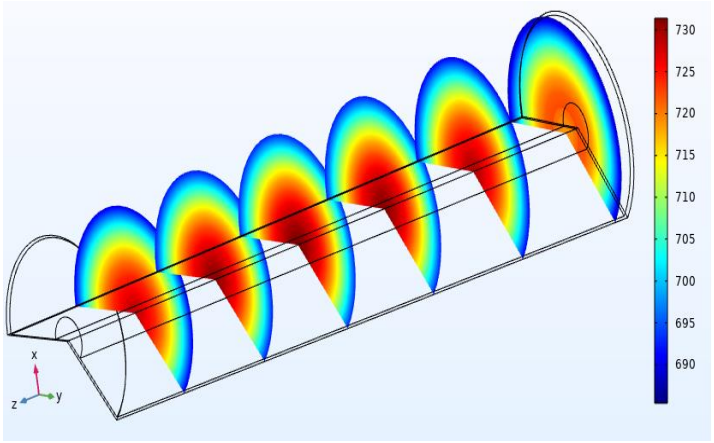


(b) Temperature distribution (Slices) at $C_r = 10$, $t = 300$ , $SOC_i = 0.5$, and $I_{\text{app}} = 25$

**Figure 6.** 3D Temperature distribution in the battery at $t = 3600$.

*6.1. Constant Current Discharge*

Discharge curves at fixed power, when both the cell current and voltage change, are necessary to execute the constant current discharge of lithium-ion batteries. The $C_r$ is a measurement used to determine the current rate of the charging or discharging process to estimate or specify the expected life and productivity of a lithium-ion cell. This differs from the traditional approach of determining battery performance, in which the current is stable, but the voltage and power are changeable. That is because the polarization voltage in the electrode processes rises with higher discharge currents, while the voltage during discharge is reduced [**42**]. The battery gets depleted in the following phases in this simulation: the first full discharge with a continuous current, the battery is completely depleted. While the second discharge was halted when the cell potential fell below 3.9 V. The test was carried out at a 25°C ambient temperature and a wide variety of $C_r$ to demonstrate the change in battery temperature, as shown in Table 2. Figure 7 indicates that when the charge/discharge rate is raised, the temperature tracking becomes more accurate, indicating that draining at a typical pace is desirable since fast charge/discharge has a negative influence on cell lifetime.

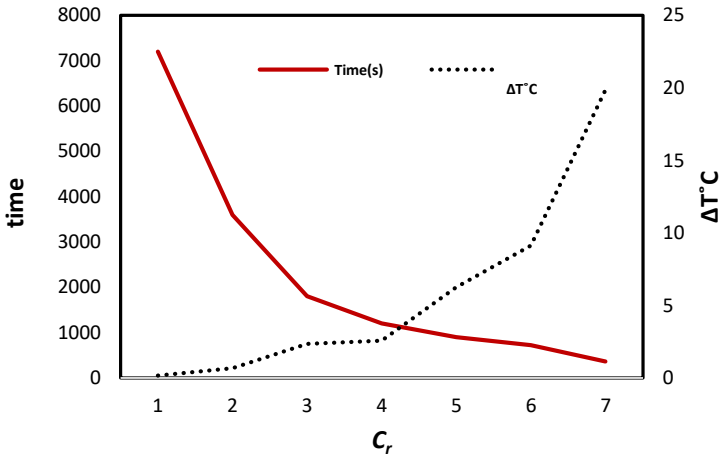


**Figure 7.** Temperature and time at different values of $C_r$

As shown in Figure 7, when the $C_r$ increases at a uniform ambient temperature in all cases, Battery temperature increases gradually. High discharge rates cause rapid changes in the volume of lithium ions, breaking the SEI layer and stimulating further electrolyte decomposition, thus further capacity loss where the SEI layer or solid-electrolyte separator layer is a component of lithium-ion batteries, which consists of the electrolyte-linked decomposition materials in the battery and that ions pass through it during charging and recharging at the molecular level, Also due to the increase in the internal resistance of the battery in the event of an increase in the rate of charging and discharging, which leads to an increase in the temperature of the battery.

*6.2. State of Charge*

The capacity that is currently accessible as a function of the rated capacity is denoted by the state of charge (SOC) of a cell. Because determining the SOC of battery is a difficult process that varies based on the battery type and application, considerable development and research have been done in recent

years to enhance SOC estimate accuracy. One of the key duties of battery management systems is accurate SOC estimate, which will assist increase system performance and dependability while also extending the battery's lifetime.

**Table 3.** Different values of SOC

| $C_r$ | Time (s) | T ˚C | ΔT ˚C | T ˚C | ΔT ˚C | T ˚C | ΔT ˚C |
|---|---|---|---|---|---|---|---|
| | | SOC = 100% | | SOC = 50% | | SOC = 0% | |
| 0.5 | 7200 | 25.58 | 0.58 | 25.24 | 24.66 | 28.21 | 3.55 |
| 1 | 3600 | 26.51 | 1.51 | 25.79 | 25.21 | 33.6 | 8.94 |
| 2 | 1800 | 30.5 | 5.5 | 27.47 | 26.89 | 45.85 | 21.19 |
| 3 | 1200 | 35.85 | 10.85 | 29.8 | 29.22 | 59.85 | 35.19 |
| 4 | 900 | 40.85 | 15.85 | 30.16 | 29.58 | 57.85 | 33.19 |
| 5 | 720 | 46.85 | 21.85 | 32.93 | 32.35 | 85.85 | 61.19 |
| 10 | 360 | 74.85 | 49.85 | 59.85 | 59.27 | 42.85 | 18.19 |

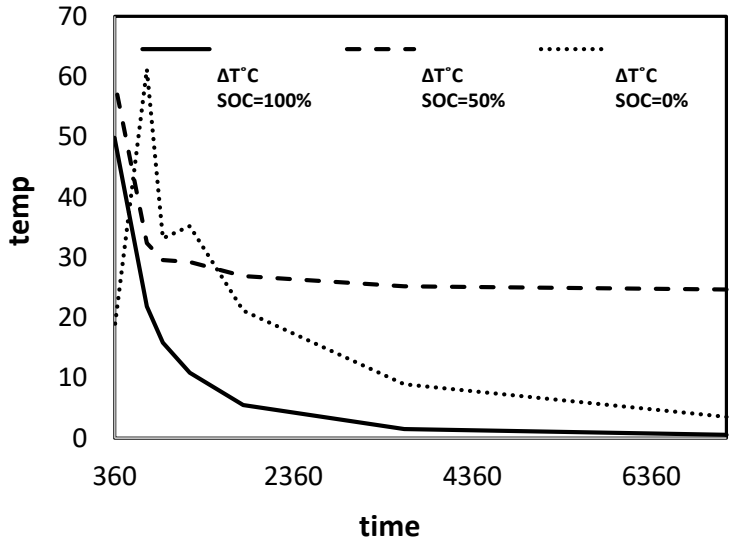


**Figure 8.** The temperature of the battery at different values of SOC

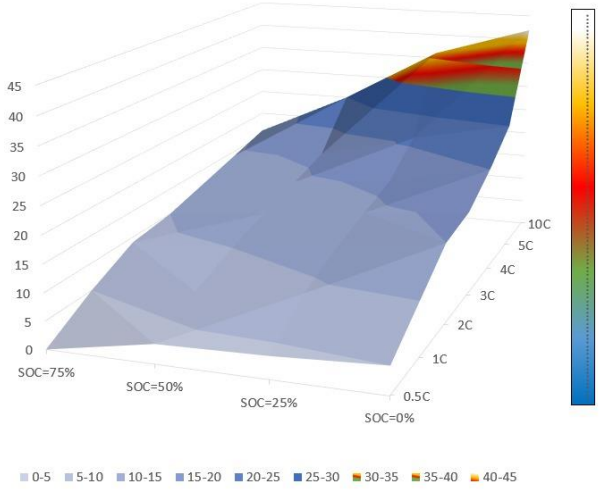


**Figure 9.** The shaded plot of temperature at different values of SOC

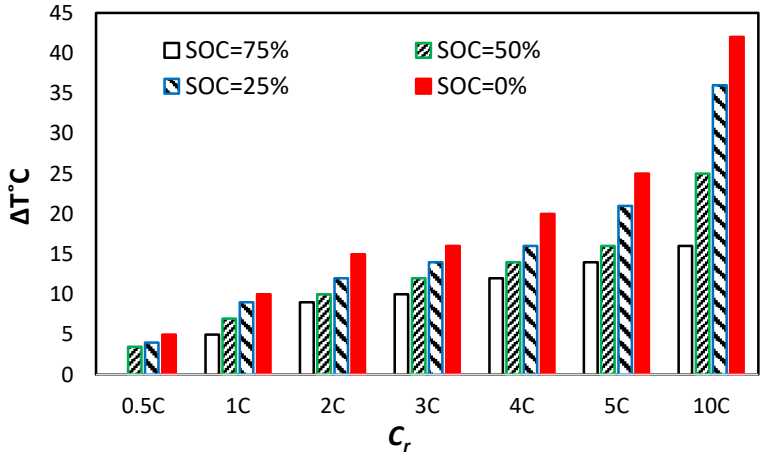


**Figure 10.** The temperature of the battery at different values of SOC and $C_r$

In reality, accurate battery SOC prediction helps prevent unplanned system outages and prevents batteries from being overcharged or drained, which can cause lasting harm to the internal structure of the battery. However, because battery discharge and charge entail complicated chemical and physical processes, it is not possible to do so. The value of the SOC varies from 0% to 100%. If the SOC is 100 percent, the cell is fully charged, whereas a SOC of 0 percent indicates that the cell is completely drained. SOC stands for the state of charge, and it is the most crucial metric in the battery management system since it provides the foundation for everything else. As a result, its precision and resilience are critical, and it is mostly used to reflect the battery's remaining capacity, which is numerically distinct as the relation of remaining capacity to battery capacity, with a value range of 0 to 1. The thermal performance of the cell is examined in this study at various SOCs. It is noticed that when SOC decreases the battery temperature increases or the battery surface temperature rises during discharge, especially at low SOC with increasing of $C_r$ as illustrated in Table 3 and Figures (8-10). The temperature increase is caused by the battery's loss of original energy as heat. As shown in figure.9, 10, we notice that with the increase in the rate of charging and discharging and the decrease in the SOC of the battery, a noticeable rise in the temperature of the battery results, due to the amount of work done to charge the battery at a full rate, and this depends on the state of charging the battery if it is satisfied by 75%, 50%, 25% or 0%, as the lower the rate Charging increased the rate of temperature rise.

*6.3. Entropic Heat Coefficient*

Heat production in lithium titanate oxide cells is a complicated procedure that necessitates knowledge of how electrochemical reaction rates vary along with time and temperature. To create an accurate and useful thermal model, researchers need a thorough grasp of the entropic heat coefficient. To compute heat production, the coefficient of entropic heat must be established. Is among the most popular significant parameters impacting the quantity of reversible heat is the entropic heat coefficient [**43-45**]. The potentiometric and calorimetric techniques are two approaches for measuring the entropy shape of a cell. The potentiometric approach is used to measure the battery's open-circuit voltage at various temperatures, which is a time-consuming procedure. The open-circuit potential has a linear relationship with the battery temperature, and the slope of this linear relationship is the entropic coefficient $dU/dT$. The calorimetric approach, in addition to the potentiometric method, is another way

to assess entropy change. The calorimeter used in the battery application was created to assess total heat generation, and it comes in two flavors: accelerating rate and isothermal heat conduction calorimeters. Because the calorimeter can barely detect overall heat production, further measurements are needed to distinguish between reversible and irreversible heat [**46**].

**Table 4.** Effect of different values of $h$

| $h$ [W.m$^2$.k] | 5 | 10 | 15 | 20 | 25 | 50 |
|---|---|---|---|---|---|---|
| $T$ ˚C | 27.2 | 26.3 | 25.9 | 25.54 | 25.57 | 25.31 |
| $\Delta T$ ˚C | 0.16 | 0.66 | 2.35 | 2.57 | 6.26 | 9.12 |

The goal of this research is to look into the impacts of different factors on the entropic coefficient of lithium titanate oxide cells. The status of charge levels was examined in setting an alternating charge/discharge current at 1C, and the battery is charged to a 20% initial level of charge. Temperatures range from 20 to 70 degrees Celsius, with voltages ranging from 3.8 to 4.2 volts. In the different researches observing their relationship between the ambient temperature and the coefficient heat transfer of the battery, the heat transfer model which used in the previous result $h = 20\ [W.m^2.k]$ but in this study, simulation results with different heat transfer coefficient values (5, 10, 15, 20, 25, 50) $[W.m^2.k]$ are obtained, the heat transfer coefficient in the internal battery is very low and is related to the cooling fan in the battery module and requires a cooling fan with greater power or different cooling material types.

Equation (9) gives the relation between the power of the battery $q_0$, the heat transfer coefficient $h$, and the change among the external temperature $T_{ext}$ and the inlet temperature $T$. From the obtained results, it is noticed that the temperature rises with the increase of heat transfer coefficient as shown in Table 4 and Figure 11, so it is interesting to continue to study the effect of value $h = 50\ [W.m^2.k]$ to achieve the best result. As a result of the simulation of different values of the heat transfer coefficient at a constant ambient temperature, it was found that when the heat transfer rate increases, the battery temperature decreases. This was done to clarify the best value of the heat transfer coefficient in the case of the battery with the previous specifications and parameters.

$$q_0 = h.(T_{ext} - T) \tag{9}$$

*6.4. Thermal Conductivity*

Thermal conductivity is a metric that has a big impact on the spatial temperature rises of lithium-ion cells while they're in operation or when they're abused. It has an impact on the cell's ability to dissipate the heat created in a regular process or when thermal escaped propagates transferring from one cell to the next following an outside short circuit. As a result, thermal conductivity is an important metric to be considered when evaluating the protection of a Li-ion cell [**47**]. This section emphasizes the need for precise thermal conductivity monitoring of Li-ion cells when investigating the thermal behavior of lithium-ion cells throughout their whole product life. Making gradual modifications to the cell cooling

structure based on the aging state can aid in the avoidance of a premature thermal runaway. Thermal conductivity influences the dissipation of heat produced by a battery through regular operation and is LIBs thermal characteristic if it varied improving in thermal properties, so in this study, variable values of the thermal conductivity are investigated. According to Equation (10), the effect of thermal conductivity can be investigated.

$$\frac{\delta}{\delta x}\left(k\frac{\delta T}{\delta x}\right)+\frac{\delta}{\delta y}\left(k\frac{\delta T}{\delta y}\right)+\frac{\delta}{\delta z}\left(k\frac{\delta T}{\delta z}\right)+q=\rho C_p\frac{\delta T}{\delta t} \tag{10}$$

where the thermal conductivity is *k* dependent on cartesian coordinates x, y, and z, the temperature is $T$ [K] in a certain coordinate $(x,y,z)$ within the medium, the specific heat capacity is $C_p$ $(J.kg^{-1}.k^{-1})$ the mass density is $\rho$ and the heat transfer rate per unit of volume is $q$ and time *t* in second (s). The distribution of temperature, $T(x,y,z)$, as a function of time can be achieved from its solution. In this search study, the results at different values of thermal conductivity (0.339, 0.356, 0.373, 0.39, 1.407, 1.339, 3.339, 4.407, 7.339, 12.407 $W.m^{-1}.k^{-1}$) are obtained. It is noticed from the result in the Table.5, Figure.12 shows the temperature reduction with increasing the thermal conductivity but in lower limiting and with increasing value of thermal conductivity the temperature of the cell is stable at a certain amount. In the case of studying the thermal conductivity of the battery between small, medium, and large values, a decrease in the rate of temperature rise is observed when the thermal conductivity of the battery increases, but the increase comes in a relative and slight case 1 as a model.

**Table 5.** Effect of different values of thermal conductivity

| $k$ [w·m$^{-1}$·k$^{-1}$] | 0.339 | 0.356 | 0.373 | 0.39 | 1.339 | 1.407 | 3.339 | 4.407 | 7.339 | 12.407 |
|---|---|---|---|---|---|---|---|---|---|---|
| $T$ ˚C | 25.23 | 25.23 | 25.23 | 25.23 | 25.18 | 25.18 | 25.17 | 25.17 | 25.17 | 25.17 |
| $\Delta T$ ˚C | 0.23 | 0.23 | 0.23 | 0.23 | 0.18 | 0.18 | 0.17 | 0.17 | 0.17 | 0.17 |

*6.5. Heat Capacity*

Due to differences in materials, internal structures, and manufacturing techniques, the specific heat capacity of various batteries can vary significantly. Furthermore, batteries have a complicated chemical composition, and during charging, discharging, and aging, complex chemical reactions occur in the battery, resulting in a change in chemical composition and phase structure on the electrodes. As a result, State of charge (SOC), State of Health (SOH), temperature, and other factors will alter the battery's particular heat capacity. The battery's particular heat capacity is a critical factor in the development of the thermal model, and it is influenced by a variety of factors such as SOC, temperature, etc. A battery's specific heat capacity can be measured in a variety of methods. The findings of several measurement methods are not the same. Equation 11 shows the relationship between the diverted of temperature and heat capacity $C_p$ $[J/kg.k]$ and is affected by many factors such as temperature and SOC. In order to calculate the external coefficient of heat transfer $(h)$ of the assembly the following energy balance has been utilized as:

$$\dot{Q}+hA\left(T-T_i\right)=mC_p\left(\frac{dT}{dt}\right) \tag{11}$$

where $\dot{Q}$ is the heat supplied by the heater, $m$ is the mass of active material, ($T_i$) is the initial temperature (i.e. ambient temperature), $T$ is the battery temperature, $A$ is the area surface $C_p$ is the heat capacity. The result in Table.6 that no change value of the battery temperature in these values as shown. Note that after doing a lot of simulation operations of the model, each temperature has a specific heat capacity to get the best results for the thermal battery condition.

**Table 6.** Effect of various values of heat capacity on the temperature

| Temperature $T$ ˚C | 30 | 35 | 40 | 45 | 50 |
|---|---|---|---|---|---|
| Specific Heat Capacity $C_p$ | 0.85 | 0.0 | 0.84 | 0.81 | 0.84 |

*6.6. Thermal Energy Density*

Understanding heat production and movement inside the battery is critical for regulating the internal battery temperature. Inadequate thermal transfer within the battery, even with a powerful external BTMS, can result in a significant internal temperature rise and a large internal temperature gradient, especially as the battery's energy density and charge rate increase. As a result, for LIBs designed for high energy density and rapid charging, a detailed examination of the optimal thermal conditions, thermal phenomena (i.e., heat generation and movement) inside the battery, and BTMS are necessary. Using thicker electrodes to improve the areal loading of active materials is an efficient approach to boosting the energy density of LIBs. The thermal energy density parameter is connected by the redial dimension models the effect of particle size on the li-ion distribution within the electrodes by calculating the time-dependent ion concentration distribution as in Equation (12).

$$\frac{dC}{dt} = \frac{1}{r^2} \cdot \frac{d}{dr}\left(D_s \cdot r^2 \cdot \frac{dC}{dr}\right) \quad (12)$$

where $\boldsymbol{C}$ is the concentration of li-ion, $\boldsymbol{D_s}$ is the thermal density and $\boldsymbol{r}$ is the particle radius of li-ion, so density rise with increasing concentration of li-ion. But study thermal behavior for li-ion battery in different value of density parameter. From the obtained results shown in Table 7, Figure 13, it is noticed that there is a decrease in the battery temperature concerning the inlet temperature with decreasing the values of density. In this study, all the parameters in certain values in various discharge ratios are investigated to get the suitable temperature of the battery. Effect of different values of the thermal energy density is the stability in this values: 1114.6,1126.3,1138.3,1150.2 but the stability with negative, it's the battery temperature is lower than the ambient temperature until it reaches a value 1160.6 the value of battery temperature rises with 0.17 degree for ambient temperature.

**Table 7.** Effect of different values of the thermal energy density

| $D$ [kg/m$^3$] | 1114.6 | 1126.3 | 1138.3 | 1150.2 | 1160.6 |
|---|---|---|---|---|---|
| $T$ ˚C | 16.19 | 16.19 | 16.19 | 16.19 | 25.17 |
| $\Delta T$ ˚C | -8.81 | -8.81 | -8.81 | -8.81 | 0.17 |

Finally, a study of the batteries in more than one case was performed when the values of the thermal parameters were changed according to the previous study and when a series of changes to these variables like as (specific heat capacity, thermal conductivity, thermal energy density) and spikes in different charge/discharge rates (0.5, 1, 1.5, 2, 2.5 C). From the obtained results, it is found that through the rise of discharge/charge rate in the battery and the increase of thermal conductivity and heat capacity with decreasing thermal energy density, the best case is obtained, as shown with no. 5 concerning other cases mentioned in Table 8, in terms of the temperature differential between the battery temperature and the ambient temperature, this is true. From figure 14 and Table 8 it is noticed that the fifth case is the best one, because it records the lowest temperature.

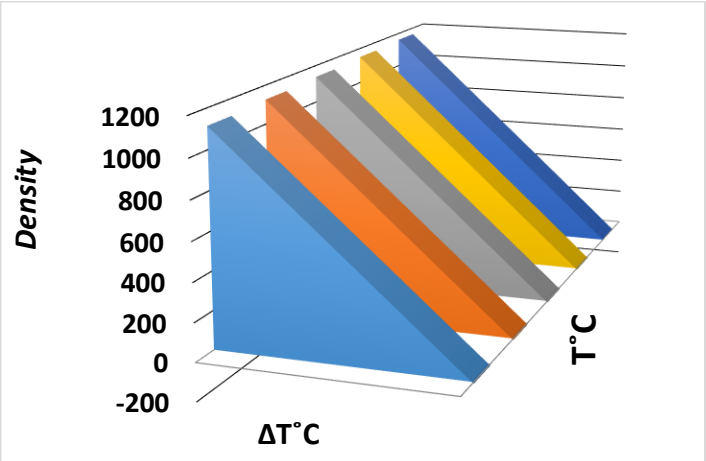


**Figure 13.** The temperature of the cell at the diverse thermal energy density

**Table 8.** Suggested cases

| Parameter Description | Case.1 | Case.2 | Case.3 | Case.4 | Case.5 |
|---|---|---|---|---|---|
| Charging & discharging battery rate $C_r$ | 0.5 | 1.0 | 1.5 | 2.0 | 2.5 |
| Heat capacity of battery $C_{pB}$ | 3270.0 | 3330.0 | 3410.0 | 3480.0 | 3560.0 |
| Resistivity of battery $r_{ho\_B}$ | 1160.6 | 1150.2 | 1138.3 | 1126.3 | 1114.6 |
| Thermal conductivity of separator $k_{T\_s}$ | 339 | 356 | 373 | 390 | 407 |
| Temperature of Battery $T$_batt | 27.58 | 28.35 | 27.24 | 26.66 | 26.33 |

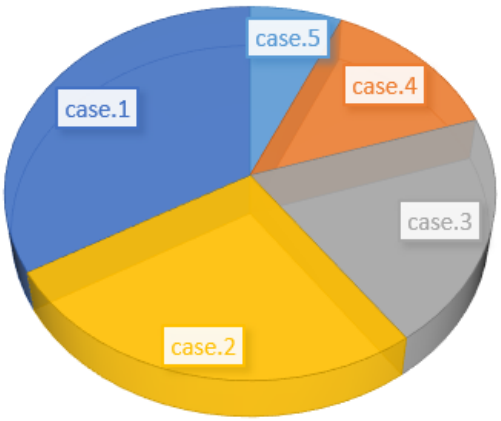


**Figure 14.** Comparison between the results of the suggested cases

## 7. CONCLUSION

In this paper, the cylindrical type of the lithium-ion cell was simulated using a simulation technique based on the finite element method with coupling both the thermal and chemical models of the cell. That to study the behavior of the cell in different cases of charging and discharge, at multiple SOC and as well as to study its thermal performance at different values of its thermal parameters such as heat transfer coefficient, thermal conductivity, heat capacity, and density. The thermal behavior of LIBs was found to be impacted by the state of charge of the battery SOC and $C_r$, based on the findings. It is noticed that when the discharging/charging rate increases the temperature also increases. Also, it is seen that the temperature rises with the rise of some parameters such as density and it decreases with the increase of some parameters such as heat capacity, thermal conductivity, and heat transfer coefficient. Finally, according to the results obtained from different cases under study, the best case was mentioned.

ACKNOWLEDGMENT
The authors appreciatively recognize the Egyptian Science and Technology Development Fund (STDF) for subsidizing this work among the STDF project with ID no. 43247.

## References

1. C. Xiang, C.W. Wu, W.X. Zhou, G. Xie and G. Zhang, *Front. Phys*., 17 (2022) 13202.
2. M. Armand and J.M. Tarascon, *Nature*, 451 (2008) 652.
3. V. Etacheri, R. Marom, R. Elazari, G. Salitra and D. Aurbach, *Energy Environ. Sci.*, 4 (2011) 3243.
4. J.B. Goodenough and K.S. Park, *J. Am. Chem. Soc*., 135 (2013) 1167.
5. A. El-Tayeb, A.H. El-Shazly, M.F. Elkady and A. Abdel-Rahman, *Plasma Phys. Rep*., 42 (2016) 887.
6. J.M. Tarascon and M. Armand, *Nature*, 414 (2001) 359.
7. K. Shah, V. Vishwakarma and A. Jain, *ASME J. Electrochem. Energy Convers. Storage*, 13 (2016) 030801.
8. H. Lundgren, P. Svens, H. Ekström, C. Tengstedt, J. Lindström, M. Behm and G. Lindbergh, *J. Electrochem. Soc*., 163 (2015) A309.
9. J. Kim, J. Oh and H. Lee, *Appl. Therm. Eng*., 149 (2019)192.
10. R. Wang, Z. Liang, M. Souri, M.N. Esfahani and M. Jabbari, *Int. J. Heat Mass Transfer*, 183 (2022) 122095.
11. A.A. Pesaran, *J. Power Sources*, 110 (2002) 377.
12. B. Li, X. Li, X. Bai and Z. Li, *J. Mod. Power Syst. Clean Energy*, 6 (2018) 1234.
13. M.H. Amini and O. Karabasoglu, *Energies*, 11 (2018)196.
14. A. Li, A.C.Y. Yuen and W. Wang, *Molecules*, 26 (2021) 478.
15. D.E. Stephenson, E.M. Hartman, J.N. Harb and D.R. Wheeler, *J. Electrochem. Soc*., 154 (2007) 154.
16. I.V. Thorat, D.E. Stephenson, N.A. Zacharias, K. Zaghib, J.N. Harb and D.R. Wheeler, *J. Power Sources*, 188 (2009) 592.
17. H.D.T.G. Samarasinghe, S. Lewis and M. Kazilas, Thermal and Heat Transfer Modeling of Lithium –Ion Battery Module during the Discharge Cycle, COMSOL Conference Paper Version1.2, London, United Kingdom, 2020, 1-6.
18. J.M. Sherfey and A. Brenner, *J. Electrochem. Soc*., 105 (1958) 665.
19. S. Gross, *J. Energy Cons*., 9 (1969) 55.
20. A. Dibrov and V.A. Bykov, *J. Appl. Chem*., 2025 (1977) 49.

21. D.M. Chen and H.F Gibbad, *J. Electrochemical and Sci*., 1975 (1983) 130.
22. X. Li, F. He and L. Ma, *J. Power Sources*, 238 (2013) 395.
23. A. El-Tayeb, A.H. El-Shazly, M.F Elkady and A. Abdel-Rahman, *Desalin. Water Treat*., 61 (2017) 230.
24. Z. Bi, Finite Element Analysis Applications: A Systematic and Practical Approach, Academic Press, (2018) London, UK.
25. J. Tu; G.H. Yeoh and C. Liu, Computational Fluid Dynamics: A Practical Approach, Butterworth-Heinemann, (2018) Oxford, UK.
26. T.B.Y. Chen, A.C.Y. Yuen, G.H. Yeoh, W. Yang and Q.N. Chan, *Fire*, 2 (2019), 1.
27. A.C. Yuen, G.H. Yeoh, V. Timchenko, S.C. Cheung, Q.N. Chan and T. Chen, *Int. J. Comput. Fluid Dyn.*, 31 (2017) 324.
28. L. Spitthoff, P.R. Shearing and O.S. Burheim, *Energies*, 14 (2021) 1248.
29. S.C. Chen, Y.Y. Wang and C.C. Wan, *J. Electrochem. Soc*., 153 (2006) A637.
30. P.M. Gomadam, R.E. White and J.W. Weidner, *J. Electrochem. Soc*., 150 (2003) A1339.
31. L. Song, Y. Zheng, Z. Xiao, C. Wang and T. Long, *J. Electron. Mater*., 51 (2022) 30.
32. T. Yamanaka, Y. Takagishi, Y. Tozuka and T. Yamaue, *J. Power Sources Adv*., 416 (2019) 132.
33. D. Ouyang, M. Chen, J. Liu, R. Wei, J. Weng and J. Wang, *RSC Adv*., 8 (2018) 33414.
34. M. Ghiji, S. Edmonds and K. Moinuddin, *Appl. Sci*., 11 (2021) 1247.
35. A. El-Tayeb, A.H. El-Shazly and M.F. Elkady, *Energies* 9 (2016) 874.
36. L.H. Saw, Y. Ye and A.A.O. Tay, *Energy Convers. Manage*., 87 (2014) 367.
37. B.A. Johnson and R.E. White, J. *Power Sources*, 70 (1998) 48.
38. D. Djian, F. Alloin, S. Martinet, H. Lignier and J.Y. Sanchez, *J. Power Sources*, 172 (2007) 416.
39. R. Korthauer, Lithium-Ion Batteries: Basics and Applications, Springer, (2018) Berlin, Germany.
40. G. Liu and L. Zhang, *World Electr. Veh. J.*, 12 (2021) 250.
41. A. El-Tayeb, A.H. El-Shazly, M.F. Elkady and A. Abdel-Rahman, *Contrib. Plasma Phys*., 56 (2016) 855.
42. W. Lance,. Traub, *Batteries*, 2 (2016) 17.
43. S.S. Madani, E. Schaltz and S. Kaer, *Energies*, 12 (2019) 2685.
44. F. Geifes, C. Bolsinger, P. Mielcarek and K.P. Birke, J. *Power Sources*, 419 (2019) 148.
45. Z. Geng, J. Groot and T. Thiringer, *IEEE Trans. Transp. Electrif*., 6 (2020) 257.
46. A. El-Tayeb, A.Z. El-Dein, A.Y. Elnaggar and E.E. Hussein, *Sustainability*, 13 (2021)12971.
47. G. Kovachev, A. Astner, G. Gstrein, L. Aiello, J. Hemmer, W. Sinz and C. Ellersdorfer, *Batteries*, 7 (2021) 42.